

Ultrafast erbium-doped fiber laser mode-locked by a CVD-grown molybdenum disulfide (MoS₂) saturable absorber

Handing Xia, Heping Li,* Changyong Lan, Chun Li, Xiaoxia Zhang, Shangjian Zhang and Yong Liu

State Key Laboratory of Electronic Thin Films and Integrated Devices, School of Optoelectronic Information, University of Electronic Science and Technology of China, Chengdu 610054, China

*oehpli@uestc.edu.cn

Abstract: We demonstrate an erbium-doped fiber laser passively mode-locked by a multilayer molybdenum disulfide (MoS₂) saturable absorber (SA). The multilayer MoS₂ is prepared by the chemical vapor deposition (CVD) method and transferred onto the end-face of a fiber connector. Taking advantage of the excellent saturable absorption of the fabricated MoS₂-based SA, stable mode locking is obtained at a pump threshold of 31 mW. Resultant output soliton pulses have central wavelength, spectral width, pulse duration, and repetition rate of 1568.9 nm, 2.6 nm, 1.28 ps, and 8.288 MHz, respectively. The experimental results show that multilayer MoS₂ is a promising material for ultrafast laser systems.

©2014 Optical Society of America

OCIS codes: (140.3510) Lasers, fiber; (140.4050) Mode-locked lasers; (160.4236) Nanomaterials; (190.7110) Ultrafast nonlinear optics.

References and links

1. U. Keller, "Recent developments in compact ultrafast lasers," *Nature* **424**(6950), 831–838 (2003).
2. W. Sibbett, A. A. Lagatsky, and C. T. Brown, "The development and application of femtosecond laser systems," *Opt. Express* **20**(7), 6989–7001 (2012).
3. Q. L. Bao, H. Zhang, Y. Wang, Z. H. Ni, Y. L. Yan, Z. X. Shen, K. P. Loh, and D. Y. Tang, "Atomic-layer graphene as a saturable absorber for ultrafast pulsed lasers," *Adv. Funct. Mater.* **19**(19), 3077–3083 (2009).
4. F. Bonaccorso, Z. Sun, T. Hasan, and A. Ferrari, "Graphene photonics and optoelectronics," *Nat. Photonics* **4**(9), 611–622 (2010).
5. S. Yamashita, "A tutorial on nonlinear photonic applications of carbon nanotube and graphene," *J. Lightwave Technol.* **30**(4), 427–447 (2012).
6. D. Popa, Z. Sun, F. Torrisi, T. Hasan, F. Wang, and A. Ferrari, "Sub 200 fs pulse generation from a graphene mode-locked fiber laser," *Appl. Phys. Lett.* **97**(20), 203106 (2010).
7. L. M. Zhao, D. Y. Tang, H. Zhang, X. Wu, Q. L. Bao, and K. P. Loh, "Dissipative soliton operation of an ytterbium-doped fiber laser mode locked with atomic multilayer graphene," *Opt. Lett.* **35**(21), 3622–3624 (2010).
8. Z. Sun, T. Hasan, F. Torrisi, D. Popa, G. Privitera, F. Wang, F. Bonaccorso, D. M. Basko, and A. C. Ferrari, "Graphene mode-locked ultrafast laser," *ACS Nano* **4**(2), 803–810 (2010).
9. G. Sobon, J. Sotor, I. Pasternak, A. Krajewska, W. Strupinski, and K. M. Abramski, "Thulium-doped all-fiber laser mode-locked by CVD-graphene/PMMA saturable absorber," *Opt. Express* **21**(10), 12797–12802 (2013).
10. Y. Cui and X. Liu, "Graphene and nanotube mode-locked fiber laser emitting dissipative and conventional solitons," *Opt. Express* **21**(16), 18969–18974 (2013).
11. X. L. Qi and S. C. Zhang, "Topological insulators and superconductors," *Rev. Mod. Phys.* **83**(4), 1057–1110 (2011).
12. H. Yu, H. Zhang, Y. Wang, C. Zhao, B. Wang, S. Wen, H. Zhang, and J. Wang, "Topological insulator as an optical modulator for pulsed solid-state lasers," *Laser Photon. Rev.* **7**(6), L77–L83 (2013).
13. H. Zhang, C. X. Liu, X. L. Qi, X. Dai, Z. Fang, and S. C. Zhang, "Topological insulators in Bi₂Se₃, Bi₂Te₃ and Sb₂Te₃ with a single Dirac cone on the surface," *Nat. Phys.* **5**(6), 438–442 (2009).
14. F. Bernard, H. Zhang, S. P. Gorza, and P. Emplit, "Towards mode-locked fiber laser using topological insulators," in *Nonlinear Photonics*, OSA Technical Digest (online) (Optical Society of America, 2012), paper NTh1A.5.
15. C. Zhao, H. Zhang, X. Qi, Y. Chen, Z. Wang, S. Wen, and D. Tang, "Ultra-short pulse generation by a topological insulator based saturable absorber," *Appl. Phys. Lett.* **101**(21), 211106 (2012).

16. C. Zhao, Y. Zou, Y. Chen, Z. Wang, S. Lu, H. Zhang, S. Wen, and D. Tang, "Wavelength-tunable picosecond soliton fiber laser with Topological Insulator: Bi_2Se_3 as a mode locker," *Opt. Express* **20**(25), 27888–27895 (2012).
17. J. Sotor, G. Sobon, W. Macherzynski, P. Paletko, K. Grodecki, and K. M. Abramski, "Mode-locking in Er-doped fiber laser based on mechanically exfoliated Sb_2Te_3 saturable absorber," *Opt. Mater. Express* **4**(1), 1–6 (2014).
18. M. Jung, J. Lee, J. Koo, J. Park, Y.-W. Song, K. Lee, S. Lee, and J. H. Lee, "A femtosecond pulse fiber laser at 1935 nm using a bulk-structured Bi_2Te_3 topological insulator," *Opt. Express* **22**(7), 7865–7874 (2014).
19. Z. C. Luo, M. Liu, H. Liu, X. W. Zheng, A. P. Luo, C. J. Zhao, H. Zhang, S. C. Wen, and W. C. Xu, "2 GHz passively harmonic mode-locked fiber laser by a microfiber-based topological insulator saturable absorber," *Opt. Lett.* **38**(24), 5212–5215 (2013).
20. H. Liu, X. W. Zheng, M. Liu, N. Zhao, A. P. Luo, Z. C. Luo, W. C. Xu, H. Zhang, C. J. Zhao, and S. C. Wen, "Femtosecond pulse generation from a topological insulator mode-locked fiber laser," *Opt. Express* **22**(6), 6868–6873 (2014).
21. K. Wang, J. Wang, J. Fan, M. Lotya, A. O'Neill, D. Fox, Y. Feng, X. Zhang, B. Jiang, Q. Zhao, H. Zhang, J. N. Coleman, L. Zhang, and W. J. Blau, "Ultrafast saturable absorption of two-dimensional MoS_2 nanosheets," *ACS Nano* **7**(10), 9260–9267 (2013).
22. H. Zhang, S. B. Lu, J. Zheng, J. Du, S. C. Wen, D. Y. Tang, and K. P. Loh, "Molybdenum disulfide (MoS_2) as a broadband saturable absorber for ultra-fast photonics," *Opt. Express* **22**(6), 7249–7260 (2014).
23. S. Wang, H. Yu, H. Zhang, A. Wang, M. Zhao, Y. Chen, L. Mei, and J. Wang, "Broadband few-layer MoS_2 saturable absorbers," *Adv. Mater.* **26**(21), 3538–3544 (2014).
24. S. Najmaei, Z. Liu, W. Zhou, X. Zou, G. Shi, S. Lei, B. I. Yakobson, J.-C. Idrobo, P. M. Ajayan, and J. Lou, "Vapour phase growth and grain boundary structure of molybdenum disulphide atomic layers," *Nat. Mater.* **12**(8), 754–759 (2013).
25. Y. Yu, C. Li, Y. Liu, L. Su, Y. Zhang, and L. Cao, "Controlled scalable synthesis of uniform, high-quality monolayer and few-layer MoS_2 films," *Sci. Rep.* **3**, 1866 (2013).
26. Y. Lee, J. Lee, H. Bark, I.-K. Oh, G. H. Ryu, Z. Lee, H. Kim, J. H. Cho, J.-H. Ahn, and C. Lee, "Synthesis of wafer-scale uniform molybdenum disulfide films with control over the layer number using a gas phase sulfur precursor," *Nanoscale* **6**(5), 2821–2826 (2014).
27. F. Wang, A. G. Rozhin, V. Scardaci, Z. Sun, F. Hennrich, I. H. White, W. I. Milne, and A. C. Ferrari, "Wideband-tuneable, nanotube mode-locked, fibre laser," *Nat. Nanotechnol.* **3**(12), 738–742 (2008).
28. A. Cabasse, G. Martel, and J. L. Oudar, "High power dissipative soliton in an Erbium-doped fiber laser mode-locked with a high modulation depth saturable absorber mirror," *Opt. Express* **17**(12), 9537–9542 (2009).
29. K. F. Mak, C. Lee, J. Hone, J. Shan, and T. F. Heinz, "Atomically thin MoS_2 : a new direct-gap semiconductor," *Phys. Rev. Lett.* **105**(13), 136805 (2010).
30. L. Nelson, D. Jones, K. Tamura, H. Haus, and E. Ippen, "Ultrashort-pulse fiber ring lasers," *Appl. Phys. B* **65**(2), 277–294 (1997).
31. D. Y. Tang, L. M. Zhao, B. Zhao, and A. Q. Liu, "Mechanism of multisoliton formation and soliton energy quantization in passively mode-locked fiber lasers," *Phys. Rev. A* **72**(4), 043816 (2005).
32. F. Rana, H. L. T. Lee, R. J. Ram, M. E. Grein, L. A. Jiang, E. P. Ippen, and H. A. Haus, "Characterization of the noise and correlations in harmonically mode-locked lasers," *J. Opt. Soc. Am. B* **19**(11), 2609–2621 (2002).

1. Introduction

Ultrafast fiber lasers have attracted considerable interest due to their various practical applications in optical communication, frequency metrology, military systems and laser micromachining [1, 2]. Passive mode locking is a simple and economic method for the generation of ultrashort pulses. To date, various techniques, such as nonlinear-optical loop mirror (NOLM), nonlinear polarization rotation (NPR), semiconductor saturable absorption mirrors (SESAMs), single wall carbon nanotubes (SWCNTs) and graphene saturable absorbers (SAs), have been exploited for realizing stable passive mode locking. Thanks to the unique zero band gap and ultrafast saturable absorption properties [3–5], graphene behaves as an excellent SA and has been widely investigated for ultrashort pulse generation in a broadband absorption spectral range [6–10]. The success of graphene greatly motivates the exploration of other graphene-like two dimensional (2D) materials for practical applications. Recently, a new class of materials called topological insulators (TIs) with an insulating bulk state and gapless Dirac-type surface/edge are attracting great interest in the condensed-matter physics [11] and laser photonics [12]. Zhang et al. has reported that TIs, such as Bi_2Te_3 , Bi_2Se_3 and Sb_2Te_3 , were characterized by graphene-like electronic-band structure [13]. Since Bernad et al. first demonstrated the saturable absorption of Bi_2Te_3 TI in 2012 [14], several experimental investigations on the utilization of TI SAs for passive mode-locking and Q-switching have been presented [15–20]. Zhao et al. has experimentally reported the ultrashort pulse generation in fiber lasers mode-locked by SAs based on Bi_2Te_3

and Bi₂Se₃ TIs [15, 16]. The saturable absorption properties were performed based on the open-aperture Z-scan measurements at 1550 nm. It was found that the Bi₂Te₃ and Bi₂Se₃ TIs had high absolute modulation depth up to 95% [15] and 98% [16] respectively, and the corresponding saturation intensities were 0.48 and 0.49 GW/cm². In addition, Sotor et al. [17] has demonstrated an erbium-doped fiber laser mode-locked with a mechanically exfoliated Sb₂Te₃-based SA. The laser produced soliton pulses centered at 1558.6 nm with 1.8 ps duration and repetition of 4.75 MHz. Apart from the aforementioned TI SAs, the saturable absorption behavior of molybdenum disulfide (MoS₂) was presented by Wang et al. under femtosecond laser excitation at 800 nm, exhibiting that the MoS₂ nanosheets in dispersions have stronger saturable absorption response than graphene dispersions [21]. Zhang et al. firstly demonstrated the generation of dissipative solitons in an ytterbium-doped fiber laser mode-locked by a MoS₂-based SA [22]. The few-layer MoS₂ used was synthesized by the hydrothermal exfoliation method, which had a saturable intensity of 15.9 MW/m² and modulation depth of 9.3% at 1.06 μm. Very recently, Wang et al. reported broadband few-layer MoS₂ SAs by the introduction of suitable defects, which were fabricated by the pulse laser deposition technique. Utilizing these SAs, passively Q-switched solid-state lasers were achieved at 1.06 μm, 1.42 μm and 2.1 μm [23]. The experimental results showed that the few-layer MoS₂ could be regarded as a promising broadband SA for pulsed lasers. However, so far, MoS₂ mode-locked fiber laser operating at around 1.55 μm has not yet been reported.

In this paper, we present an erbium-doped fiber laser mode-locked by a MoS₂-based SA. The chemical vapor deposition (CVD) method is employed to grow high-quality multilayer MoS₂. The mode-locker is assembled by sandwiching the MoS₂ film between two fiber connectors (FCs) with a fiber adapter. With the multilayer MoS₂-based SA, the compact all-fiber laser emits stable mode-locked soliton pulses with central wavelength, spectral width, pulse duration, and repetition rate of 1568.9 nm, 2.6 nm, 1.28 ps, and 8.288 MHz, respectively.

2. Preparation and characterization of MoS₂-based SA

MoS₂ thin films were synthesized in a tube furnace by the CVD method [24]. In a typical growth, 500 mg of MoO₃ powder was placed in the center of the furnace and 500 mg of sulfur powder was placed at the upstream. Several pieces of Si wafer with 300 nm SiO₂ were used as substrates and placed downstream. The quartz tube was evacuated to a base pressure of 0.1 Torr, and then flowed with Ar gas, which was controlled by a mass flow controller. After the pressure stabilized, the furnace was heated to 550 °C at a rate of 25 °C /min and maintained for 30 min. The sulfur powder was heated by a twisted heating belt with the temperature of 100 °C. After the deposition, the furnace was naturally cooled to room temperature.

Surface morphology and height profile of the MoS₂ thin films were obtained using CSPM 5500 atomic force microscopy (AFM). Raman spectra were measured by Renishaw 100 Raman spectrometer with 514 nm laser. Figure 1(a) shows the optical microscopy image of multilayer MoS₂ film. One can find that the thin film is continuous and uniform over a large area. The Raman spectrum of the multilayer MoS₂ is shown in Fig. 1(b). The sample exhibits two characteristic peaks, in parallel with two phonon modes: out of plane vibration of S atoms at 406 cm⁻¹, and in plane vibration of Mo and S atoms at 381 cm⁻¹, with a frequency difference of 25 cm⁻¹. The frequency difference of the two modes can be used to determine the layer thickness of MoS₂. In our result, 25 cm⁻¹ corresponds to 4-5 layers of MoS₂ [25, 26]. A typical AFM image is shown in Fig. 1(c). The thickness of the film which can be determined by the height profile in Fig. 1(d) is about 3.42 nm, corresponding to 5 layers of MoS₂.

For the transfer of multilayer MoS₂ film, PMMA was spin coated on the MoS₂ film. After 10 min baking at 100 °C, samples were immersed in hydrofluoric acid (30%) for a few seconds in order to lift off the PMMA-MoS₂ films. The PMMA-MoS₂ films were transferred to a deionized water to dilute and remove the etchant and residues. Then, the PMMA-MoS₂

film was transferred to end-face of a FC, followed by drying in air for 1 h. The PMMA was removed by acetone, isopropyl alcohol and then deionized water. The MoS₂ coated FC was connected to a clean FC with a fiber adapter to form the MoS₂-based mode locker.

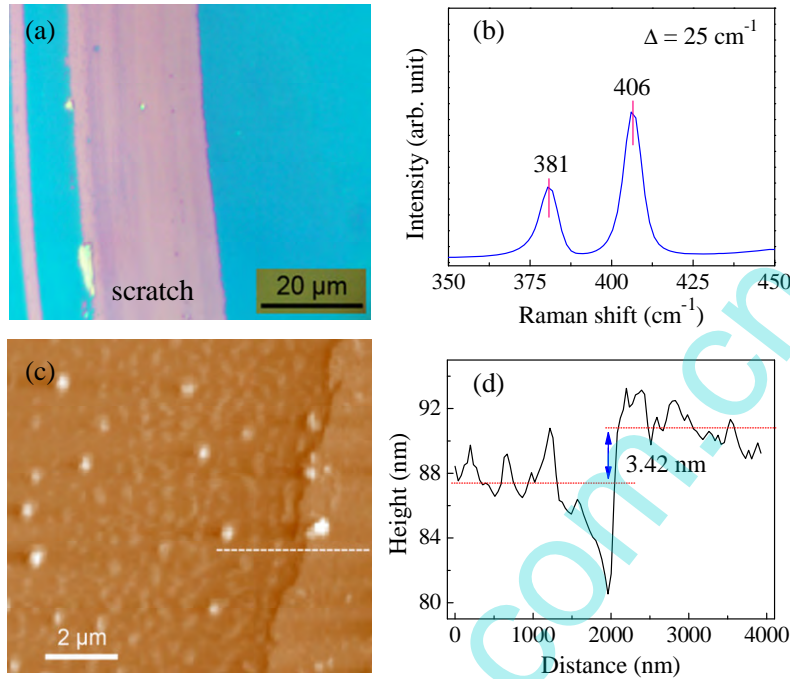


Fig. 1. (a) Optical microscopy image of a typical multilayer MoS₂ film on SiO₂ substrate. Scratch was intentionally introduced to show the color contrast between the thin film and the substrate (no MoS₂ exists in the scratched region.). (b) Corresponding Raman spectrum, (c) AFM image, and (d) AFM height profile of across the dash line in (c).

The linear absorption of the SA was measured in the range from 1525 to 1610 nm using a broadband amplified spontaneous emission (ASE) light source and an optical spectrum analyzer (Yokogawa, AQ6370C). As shown in Fig. 2(a), the linear absorption is at the level of about 71.5% and is characterized by a flat profile. Figure 2(b) schematically shows the experimental setup for the power-dependent nonlinear absorption measurement of the MoS₂-based mode locker. A commercial mode-locked fiber laser (Calmar, FPL-02CFF) operating at 1550 nm with output pulse duration of ~250 fs and repetition rate of ~20 MHz was used as input pulse source. A variable optical attenuator (VOA) was used to control input laser power. The mode-locked pulses were split by a 10/90 fiber coupler and the 10% port was used to monitor the input power, while 90% was used to pump the MoS₂-based SA. Two calibrated power meters were employed to measure the input/output power simultaneously. The experimental data for absorption α_l were then fitted according to a simple two-level SA model of $\alpha_l = \alpha_0 / (1 + I_{sat}) + \alpha_{ns}$ [3]. As shown in Fig. 2(c), the SA parameters of modulation depth α_0 , non-saturable loss α_{ns} , and saturation intensity I_{sat} were measured to be 35.4%, 34.1%, and 0.34 MW/cm², respectively. The modulation depth α_0 of our MoS₂-based SA measured at 1550 nm is much larger than that of MoS₂-based SAs at 1060 nm reported in Refs [22, 23], which may be attributed to a reason that the nonlinear absorption in a material is strongly dependent on the excitation wavelength. Moreover, the α_0 value in this work is larger than those of SWCNTs [27], multilayer graphene [3, 8] and TI-based SAs at 1550 nm [19, 20]. Experimentally, it was found that a SA with large modulation depth could effectively suppress the wave-breaking effect in a mode-locked fiber laser [28], indicating that the MoS₂ SA is potential for the generation of large energy laser pulses. To further check

whether the observed saturable absorption originated from the MoS₂ itself, we performed the power-dependent absorption measurement by replacing the MoS₂-coated FC with a common clean FC. As shown in Fig. 2(d), the measured absorption is independent of the pump peak intensity, which suggests that the observed saturable absorption of the MoS₂ SA is indeed induced by the multilayer MoS₂.

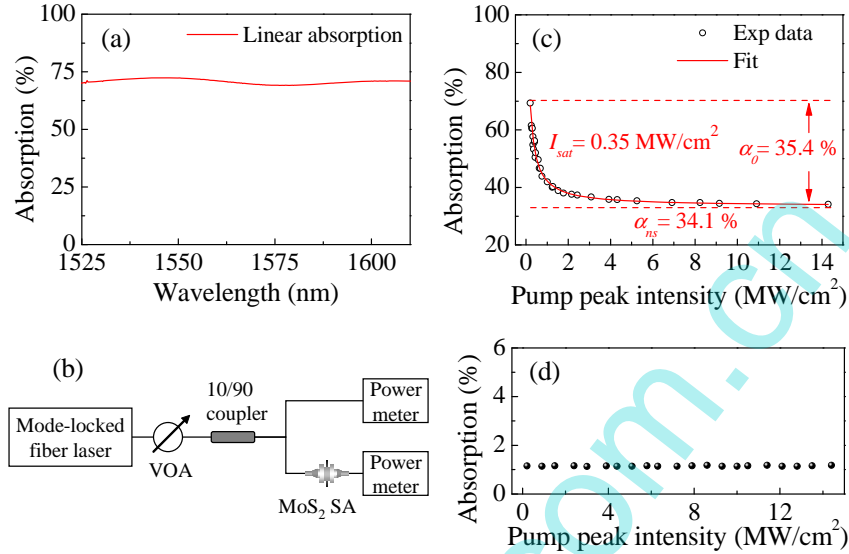


Fig. 2. (a) Linear absorption of the multilayer MoS₂-based SA. (b) Experimental setup for the power-dependent nonlinear absorption measurement. (c) Nonlinear absorption of the multilayer MoS₂-based SA. (d) Optical absorption versus pump peak intensity when the MoS₂-coated FC was replaced with a common clean FC.

It should be mentioned that the monolayer MoS₂ is a direct semiconductor with a band gap of about 1.8 eV while the multilayer MoS₂ is an indirect semiconductor with a narrow band gap of about 1.2 eV [29]. When the photons with an energy larger than the band gap, the multilayer MoS₂ can be excited by absorbing one photon. At high excitation intensities, electrons in the valance band can be easily pumped to fill the conduction band and the multilayer MoS₂ will exhibit saturable absorption due to Pauli blocking principle [21]. Wang et al. have recently demonstrated that the band gap of multilayer MoS₂ could be reduced to 0.08 eV ($\lambda = 15.4 \mu\text{m}$) by introducing suitable S defects [23]. This implies that the multilayer MoS₂ with S defects is a broadband saturable absorber. Based on the multilayer MoS₂, they have achieved passively Q-switched solid-state lasers operating at 1.06 μm , 1.42 μm and 2.1 μm . Our experimental results show that the CVD-grown multilayer MoS₂ has large saturable absorption at 1550 nm. Further investigation is needed to identify the mechanisms involved in the saturable absorption we observed.

3. Experimental setup and results

The experimental setup of the proposed fiber ring laser is schematically shown in Fig. 3(a). It has a ring cavity and the total cavity length is approximately 24.8 m. The cavity comprises of 0.8-m-long erbium doped fiber (EDF, Liekki Er80-8/125) with group velocity dispersion (GVD) of 16 ps/(nm·km), a segment of 1.0-m HI 1060 Flex fiber with GVD of 8 ps/(nm·km), and a piece of 23.0-m standard single mode fiber (SMF-28e) with GVD of 18 ps/(nm·km). The FC coated with multilayer MoS₂ (Fig. 3(b)) was spliced into the laser cavity. An optical integrated component (OIC) was used in the cavity, which has the combination functions of a wavelength-division multiplexer (WDM), an output coupler (OC), and a polarization-insensitive isolator (PI-ISO). The structure of the OIC is schematically shown in Fig. 3(c). The pump light is launched into the OIC through the port

of the pump and then reflected into the common port by the pump-reflective coating. The signal laser propagates into the OIC from the input port and partly reflected into the tap port by the 10% signal-reflective coating. The center part of the OIC is a PI-ISO which ensures the unidirectional operation. The insertion loss of the OIC was measured to be 1.7 dB at 1550 nm including the 10% output loss. A 500 mW/980 nm laser diode (LD) was used as the pump source. An in-line polarization controller (PC) was used to adjust polarization for mode-locking optimization. Through incorporating the OIC into the cavity, we greatly simplified the laser cavity configuration and reduced the insertion loss compared with a cavity using discrete components. It should be emphasized that there was no polarization sensitive component used in the laser cavity. Therefore, the effect of mode-locking by NPR was eliminated.

The laser output spectrum was observed using an optical spectrum analyzer (Yokogawa, AQ6370C). The pulse duration was measured with a commercial autocorrelator (Femtochrome, FR-103PD). The pulse train was detected by a 500-MHz digital oscilloscope (Tektronix, TDS3052C) together with a 10-GHz photodetector, whose radio frequency (RF) spectrum was measured with an 8-GHz RF spectrum analyzer (Advantest, R3267).

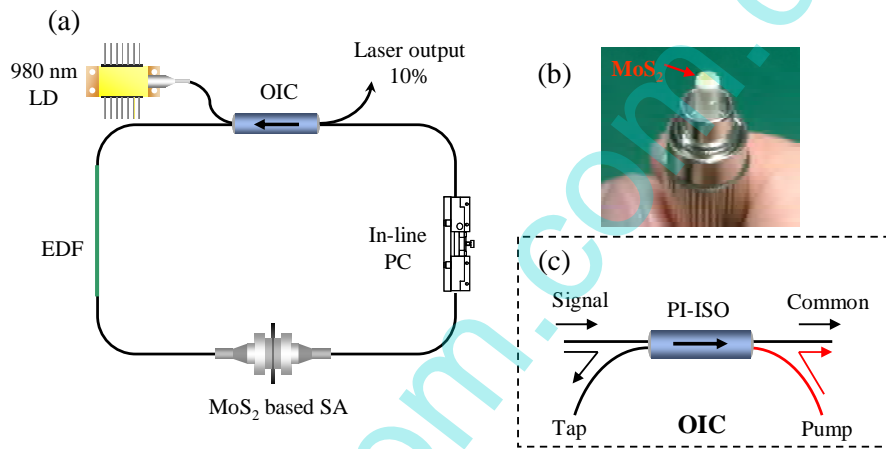


Fig. 3. (a) A schematic diagram of the fiber ring laser. 980 nm LD: 980 nm diode laser pump source, OIC: optical integrated component, EDF: erbium-doped fiber, PC: polarization controller, MoS₂-based SA: MoS₂-based saturable absorber. (b) Photograph of a FC coated with multilayer MoS₂. (c) The schematic structure of the OIC. PI-ISO: polarization-insensitive isolator

In the experiment, the continuous wave (CW) operation of the proposed laser started at a pump power of ~23 mW. When the pump power was increased to ~31 mW, the self-starting mode locking was achieved with appropriate adjustment on the PC. Figure 4(a) shows the optical spectrum of mode locked pulses. The spectrum is centered at 1568.9 nm and the 3-dB spectral width is 2.6 nm. Several pairs of sidebands are symmetrically distributed at both sides of the spectrum, which is the typical characteristic of conventional soliton pulses. A measured autocorrelation trace is shown in Fig. 4(b). It has a full width at half maximum (FWHM) width of 1.97 ps. Assuming a Sech² pulse profile, the soliton pulse duration is 1.28 ps. The time-bandwidth product (TBP) of the pulses is ~0.406, indicating that the output pulses are slightly chirped. Figure 4(c) shows the oscilloscope trace of the mode-locked pulse train. The time interval between the pulses is ~120.6 ns. Figure 4(d) presents the corresponding RF spectrum with a 2 MHz span and 3 kHz resolution bandwidth. The repetition rate of the soliton pulses is 8.288 MHz, matching exactly with the cavity roundtrip time of ~120.6 ns and the cavity length of ~24.8 m. The signal-to-noise ratio (SNR) is ~62 dB, indicating good mode-locking stability. The RF spectrum with a 100 MHz span shown in the inset of Fig. 4(d) illustrates stable operation of the pulsed laser without exhibiting a Q-switching instability. The fundamental mode locking operation was maintained up to a pump

power of ~ 152 mW. The maximum output power was 5.1 mW and the corresponding pulse energy was estimated to be 0.615 nJ.

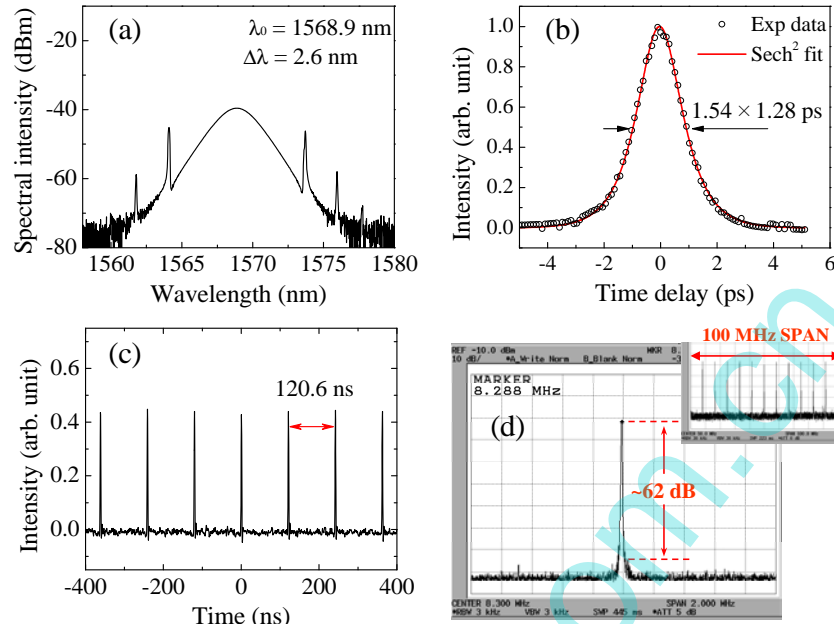


Fig. 4. Mode-locking performance of the fiber laser mode-locked by a multilayer MoS₂-based SA. (a) Optical spectrum. (b) Autocorrelation trace. (c) Pulse train. (d) RF spectrum with a 2 MHz span and 3 kHz resolution bandwidth. Inset: RF spectrum in 100 MHz span.

When the pump power was increased to 155 mW, multiple soliton operations were observed due to the soliton area theorem [30, 31]. With slight adjustment on the PC, the soliton pulses self-adjusted their positions and ultimately distributed along the cavity with an equal time interval, indicating that the harmonic mode locking (HML) operation was obtained. Figure 5(a) and 5(b) show the oscilloscope trace and RF spectrum of the 3rd HML at the pump power of 159.8 mW. The side-mode suppression ratio (SMSR) of the 3rd HML was estimated to be ~ 27 dB. The relative low SMSR could be caused by the competition between the harmonic and the fundamental mode-locking mechanisms [32]. Further investigations on the high order HML in the MoS₂ mode-locked fiber laser will be carried out in the near future.

In order to check whether the passive mode locking was attributed to the proposed MoS₂-based SA, the FC coated with multilayer MoS₂ was replaced with a common clean FC in the cavity. In this case, no mode-locked pulses were observed on the oscilloscope even if the pump power was adjusted and the PC was rotated in a wide range. This demonstrated that the saturable absorption of the MoS₂-based SA was responsible for the mode locking. To test the long-term stability of the fundamental mode locking, the laser was turned on over 8 hours in the conventional room environment. Relative fluctuations of average output power and center wavelength were $\pm 2\%$ and $\pm 0.1\%$, respectively, which indicates that the laser stably operated in the room environment.

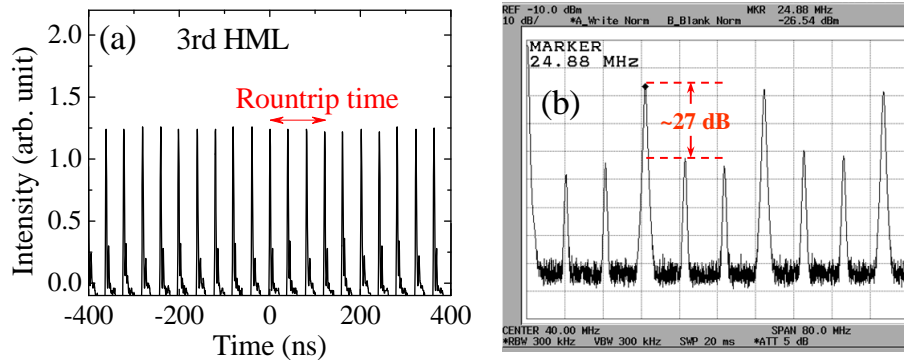


Fig. 5. (a) Output pulse train of the 3rd HML. (b) The corresponding RF spectrum

4. Conclusion

In conclusion, we have experimentally demonstrated the ultrashort pulse generation in an erbium-doped fiber laser mode-locked by a multilayer MoS₂-based SA. The multilayer MoS₂ was prepared by the CVD method and transferred to the end-face of a FC. The SA parameters of modulation depth α_0 and saturation intensity I_{sat} were measured to be 35.4% and 0.34 MW/cm², respectively. With the multilayer MoS₂-based SA, the compact all-fiber laser emitted stable mode-locked soliton pulses centered at 1568.9 nm with spectral width of 2.6 nm and pulse duration of 1.28 ps. The experimental results suggest that multilayer MoS₂ is a promising material for ultrafast laser mode locking applications.

Acknowledgments

This work was supported by the National Natural Science Foundation of China (Grant Nos. 61378028, 61106040, 61275039, and 61377037), the National Basic Research Program of China (2012CB315701) and the NCET Program (Grant No. NCET-13-0092).